Non-Homogeneous Sampling Rate Wide Area Backup Protection using Synchrophasors and IED Data

Chavez, J. J.; Kumar, N. Veera; Popov, M.; Palensky, P.; Azizi, Sadegh; Melgoza, Enrique; Terzija, Vladimir

Citation (APA)
Chavez, J. J., Kumar, N. V., Popov, M., Palensky, P., Azizi, S., Melgoza, E., & Terzija, V. (2022). Non-Homogeneous Sampling Rate Wide Area Backup Protection using Synchrophasors and IED Data. In L. Nordstrom, N. Holjevac, I. Kuzle, I. Ivankovic, M. Kezunovic, M. Paulone, H. Mohsenian-Rad, C. Muscas, & T. Basakarad (Eds.), *Proceedings of the 2022 International Conference on Smart Grid Synchronized Measurements and Analytics (SGSMA)* (pp. 1-6). Article 9806006 (2022 International Conference on Smart Grid Synchronized Measurements and Analytics, SGSMA 2022 - Proceedings). IEEE. https://doi.org/10.1109/SGSMA51733.2022.9806006

Important note
To cite this publication, please use the final published version (if applicable).
Please check the document version above.

Non-Homogeneous Sampling Rate Wide Area Backup Protection using Synchrophasors and IED Data

J. J. Chavez, N. Veera Kumar, M. Popov and P. Palensky

Faculty of EEMCS,
Delft University of Technology
Delft, The Netherlands
e-mails: j.j.chavezmuro@tudelft.nl,
N.K.VeeraKumar@tudelft.nl, M.Popov@tudelft.nl,
P.Palensky@tudelft.nl

Enrique Melgoza
Graduate Studies and Research Department
The National Technological Institute of Mexico
Morelia, Mexico
e-mail: enrique.mv@morelia.tecnm.mx

Sadegh Azizi
School of Electronic and Electrical Engineering
University of Leeds
Leeds, United Kingdom
e-mail: S.Azizi@leeds.ac.uk

Vladimir Terzija
School of Electrical Engineering,
Shandong University,
Jinan, China
email: v.terzija@skoltech.ru

Abstract— **Fault currents may result in cascading failures and even system collapse if not detected and cleared on time. To account for the possibility of failure of primary protection under stressed system conditions, an extra layer of protection is commonly employed, referred to as backup protection. This paper introduces an effective formulation for realizing remote backup protection using available data from PMUs and Intelligent Electronic Devices (IEDs). The proposed method is split into three main stages. The first stage deals with the zoning detection of the fault. The second stage is aimed at faulted line detection, and finally, the third stage determines the fault distance on the faulted line. The method is designed to take full advantage of measurements provided by PMUs and IEDs. The challenges associated with different reporting rates are resolved thanks to the dynamic decimator employed to this end. The proposed method has been implemented in real-time by applying co-simulation with MATLAB and validated using the New England IEEE 39 bus system with several fault events.**

Index Terms-- **Fault detection, Real-time simulation, Synchrophasor data, Transmission system, Wide-area backup protection.**

I. INTRODUCTION

Backup protection is designed to operate when the primary protection does not clear a fault within the required time. This is crucial to maintain power system reliability and to reduce the risk of system collapse. Based upon the design principles, the backup protection operates based on local or wide-area (remote) measurements or both. The inaccuracy of the voltage and current measurements following a fault are the major causes of failures of conventional local protection schemes [1]. The advent of PMU technology and its proliferation in power systems have paved the way for realizing backup protection using wide-area measurements. PMU data-driven methods were presented for wide-area backup protection (WABP) in [2], with the time execution larger than the primary protection. The methods are generally based on currents, which are highly distorted and can affect the accuracy of the results. Bus admittance matrix and measured voltages were proposed in [3]. Also, PMU-based algorithms can deal with highly distorted signals needed for fault detection, location and discrimination such as in [4]. WABP algorithms based on PMU data are highly accurate for fault location in [5]. The accuracy in some schemes, as in [6] depends on the number and the location of PMUs in the system. Fault-location algorithm based on fewer PMU measurements in large transmission grids was proposed in [7]. In addition, some methods can handle synchronized and unsynchronized data giving flexibility in the sampling data collection [8].

This document addresses the topic of Wide Area Backup Protection (WABP) by determining the faulted zone, line, type, direction, and distance. The data is taken from available synchrophasors and Intelligent Electrical Devices (IEDs). A data rate alteration technique is utilized based on a decimator module to overcome the different reporting rates. The method takes advantage of superimposed quantities (also known as delta quantities), the least-squares estimator (LSE) and the line characteristic equation. The technique is designed modularity and may work with a limited number of

synchronized voltage and current measurements. A set of equations are solved to identify the fault in local backup protection time limits. The main contribution of the paper can be summarized as follows:

- Fast fault detection and direction based on synchrophasor data.

- Taking advantage of both synchrophasor and IED data with different reporting rates.

- Implementation of a co-simulation environment with the potential to be used as a benchmark for future network development.

The rest of the paper is organized as follows. In Section II, an overview of the method is explained. Section III presents a case study developed in RTDS and MATLAB by applying software in the loop (SIL) that virtually represents the transmission system and the control room. Finally, the proposed method's applicability is tested using the IEEE-39 bus system. A script code automatically simulates up to 900 fault events. Section IV summarizes the conclusions of the research work.

II. METHOD OVERVIEW

Fig. 1 shows the main stages associated with the proposed method. The first stage uses synchrophasors and IED data (if available) taken from the whole network. Here, the fault is detected, and classical protection algorithms determine the phase selection and fault direction. The second stage focuses on finding the faulty zone and the faulty line. The faulty zone should be fully observable. Current and voltage phasors from IEDs and synchrophasors devices (PMUs) are used as input parameters to the linear equations to implement the LSE method and identify the faulted line. The third stage computes the fault distance in kilometers by a distributed parameter line model equation. The stages are described in detail in several subsections. The zone determination can be done randomly without any physical restrictions. The user is free to determine the best places to partition the system.

A. Step 1: Fault detection and directionality

1) Fault detection:

The main tasks of this step are fault detection, faulty phase selection, and directionality assessment.

Only the data from the synchrophasors on the boundary zone are used during this step. Thus, the signal processing becomes local. The fault is detected by Euler's numerical differentiation. The actual voltage phasor magnitude and the history of the voltage phasor magnitude are used in (1).

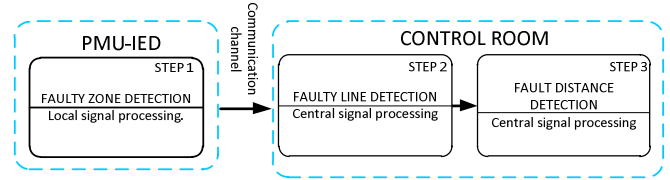$$\Delta V_{actual,A,B,C}^{k} = \frac{1}{\Delta t}\left(V_{hist,A,B,C}^{k} - V_{actual,A,B,C}^{k}\right), \quad (1)$$

Figure 1. Block overview of the proposed method

Where k corresponds to the k_{th} synchrophasor data, and Δt is the time between the history and the actual data. The historical voltage value is considered in a steady-state condition. Once the ΔV surpasses a predetermined threshold, the V_{hist} is held for all phases during the transient period. The fault is detected once $\Delta V > 0.1/\Delta t$ for three or more consecutive points. This index considers 5% error plus a safety margin of 5% for fault detection.

2) Faulty phase selection.

After the fault detection and in accordance with Fig. 2, the phase selection module is activated (SP stand for synchrophasor). The delta parameters from (1) are used in (2):

$$F_{TYPE} = round\left(\frac{\Delta V_A + \Delta V_B + \Delta V_C}{\max\left(\Delta V_A, \Delta V_B, \Delta V_C\right)}\right) \quad (2)$$
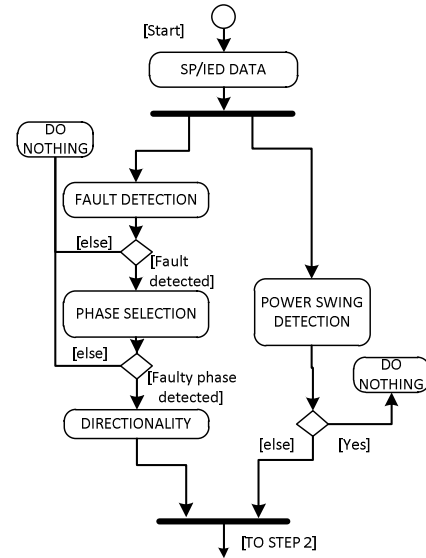

Figure 2. Method flowchart: First step fault detection and directionality.

If F_{TYPE} equals 3, 2, or 1, the fault will be declared a three-phase, two-phase, or single-phase fault, respectively [9]. Furthermore, the method can recognize an earthed fault using the zero-sequence from voltage phasors (it can also be from the current phasor). In this way, all the sets of possible faults are selected according to [9].

3) Directionality assessment

After phase selection is accomplished, the directionality process takes place. In this work, the directionality module is

based upon the technique proposed in [10], where the negative and zero sequence currents are used with a positive voltage polarization. The positive, negative and zero sequence quantities are calculated using the phasors from local PMUs or IEDs. The authors propose this method in their previous research work [11]. This can be replaced by any other effective technique that can serve the purpose of directionality identification. The proposed method is modular, which means the user can replace the fault detection, faulty phase selection, or directionality as appropriate.

4) Power swing detection

During this step, a power swing blocking module runs in parallel (see Fig.2 right-hand part). The power swing module bases its operation on the delta current quantities from continuous monitoring of the buses. The method is modified appropriately to work with phasor data [11]. The delta current (ΔI_{PS}) is computed for each cycle by:

$$\Delta I_{PS} = \left| I_{actual}^{ps} - I_{2hist}^{ps} \right|, \qquad (3)$$

Where and I_{2hist}^{ps} is the actual and two-cycle delayed current phasors, respectively. A power swing is detected when ΔI_{PS} increases monotonically by 5% or more, the steady-state value during three consecutively cycles.

The data obtained from each module is sent to the control room for further processing, as addressed in the next section.

B. Second stage: Faulted zone and faulted line determination

1) Data Rate Alteration

Synchrophasor devices make use of a common clock to synchronize the reporting data. In this sense, all data sent to the control room has the same timestamp. However, the proposed method may also use available data from IEDs, the reporting rate of which is different than that of synchrophasors provided by PMUs.

An IED uses the IEC-61850 protocol to transfer data. The communication is realized by a publisher/subscriber type with Generic Object-Oriented Substation Event (GOOSE) and Sampling Values (SV). The two protocols can send and receive data at 4000 or 4800 messages per second when used for primary protection purposes.

A fast sampling is not necessary to identify a fault because the method is proposed for backup protection. The data can be shared as 1B (Fast messages $\leq 3ms$) or 2 (Medium speed message $\leq 100ms$) [12]. As this method is intended for backup protection, a medium speed message is sufficient. To use all data effectively, the data must contain the same timestamp. A decimator is used to resample the data from IEDs and match in time with the synchrophasor data. The decimator structure is seen in Fig. 4. The decimator is highly efficient during integer or fractional sampling alteration [13].

2) Faulted Zone Determination

Once the reporting rate is synchronized, it is possible to use the fault direction data from the synchrophasors devices and IEDs at the boundaries of the zones.
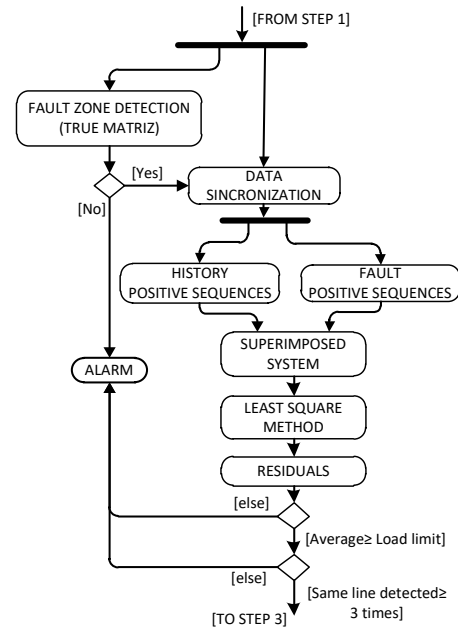

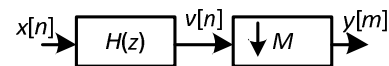Figure 3. Method Flowchart: Second step zone and line faulted detection

Figure 4. Decimator: high pass filter in series with a downsampler.

The faulty zone can be easily determined in the control room using a truth table. The truth table is a decision matrix, which uses the direction of the fault (forward or reverse). The matrix is unique for any system and zone limits. The user must decide which buses are used as zone boundaries.

3) Faulted Line Determination

The determination of the faulted line in the faulted zone is done by the superimposed value's method [1], [14], [15]. The historic positive sequence voltage and current are collected from the steady-state system condition and held for some time. The positive sequence voltage and current values are used to build a set of linear equations defining the wide-area fault locator scheme. The LSE is used to find the optimal estimator from the equations composed by the bus impedance matrices and the delta currents in all lines. The nodal equations representing the history and the actual values (fault) are:

$$V^{hist} = Z^{hist} I^{hist}; \quad V^{fault} = Z^{fault} I^{fault} \qquad (4)$$

where I is the bus injected phasor currents and V the bus phasor voltages from the faulty zone. The impedance matrix during normal conditions Z^{hist} and during the fault Z^{fault} are identical, except for the rows and columns corresponding to the line under analysis (i–j). This way, the method sweeps the zone, searching for the faulted line. The injected currents and voltage vectors of line i–j are replaced by current sources. The resulting nodal matrix from the faulty zone is:

$$\begin{bmatrix} \Delta\overline{V}_1 \\ \vdots \\ \Delta\overline{V}_{Nf} \end{bmatrix} = \begin{bmatrix} Z_{1,1}^{(i,j)} & \cdots & Z_{1,Nb}^{(i,j)} \\ \vdots & \ddots & \vdots \\ Z_{Np,1}^{(i,j)} & \cdots & Z_{Np,Nb}^{(i,j)} \end{bmatrix} \begin{bmatrix} \Delta\overline{I}_1 \\ \vdots \\ \Delta\overline{I}_{Nb} \end{bmatrix} \\ - \begin{bmatrix} Z_{1,i}^{(i,j)} & Z_{1,j}^{(i,j)} \\ \vdots & \vdots \\ Z_{Np,i}^{(i,j)} & Z_{Np,i}^{(i,j)} \end{bmatrix} \begin{bmatrix} \Delta J_{i,j} \\ \Delta J_{j,i} \end{bmatrix}, \quad (5)$$

where Np is the number of observed buses equipped with synchrophasor units and Nb denotes the number of the buses limiting with other zones. The superimposed measured positive sequence voltage and current phasors for the kth bus and the kth line are, and $\Delta\overline{I}_k = I_k^{fault} - I_k^{hist}$.

The measurements are not error-free, which is taken into account by the proposed method. An error variable ($\varepsilon_{v,k}$) is added for every kth bus voltage (5). Besides, current errors ($\varepsilon_{i,k}$) are also integrated as variables that should be accounted for, in order to form (5).

$$\Delta V_k^{meas} = \Delta\overline{V}_k + \varepsilon_{v,k}, \; \Delta I_k^{meas} = \Delta\overline{I}_k + \varepsilon_{i,k}, \quad (6)$$

The superimposed current from the k_{th} line sending end is characterized by superimposed voltage using the distributed parameter line model equation as explained in [15], [1].

$$\Delta J_k^{meas} = \sum_{q=1}^{Nb} C_{k,q}^{(i,j)} \Delta\overline{I}_q - C_{k,i}^{(i,j)} \Delta\overline{I}_{i,j} - C_{k,j}^{(i,j)} \Delta\overline{I}_{j,i} + \varepsilon_{j(k)}, \quad (7)$$

where, ΔJ_k denotes the kth line sending-end current connected to terminals u and w. The parameter C is defined as

$$C_{k,q}^{(i,j)} = \left(Z_{u,w}^c \right)^{-1} \left[\frac{Z_{u,q}^{(i,j)}}{\tanh(\gamma_{u,w}l_{u,w})} - \frac{Z_{w,q}^{(i,j)}}{\sinh(\gamma_{u,w}l_{u,w})} \right], \quad (8)$$

where $l_{u,w}$ is the line length, $Z^c_{u,w}$ is the characteristic impedance and $\gamma_{u,w}$ is the propagation constant. In this manner, by using (8) in to (5), the sending-end currents in lines can be written as a function of current injections at the limiting zone buses and the currents injected by the faulted line as:

$$\begin{bmatrix} \Delta J_1^m \\ \vdots \\ \Delta J_{Nh}^m \end{bmatrix} = - \begin{bmatrix} C_{1,i}^{(i,j)} & C_{1,j}^{(i,j)} \\ \vdots & \vdots \\ C_{Nh,i}^{(i,j)} & C_{Nh,j}^{(i,j)} \end{bmatrix} \begin{bmatrix} \Delta J_{i,j} \\ \Delta J_{j,i} \end{bmatrix} + \\ \begin{bmatrix} C_{1,1}^{(i,j)} & \cdots & C_{1,Nb}^{(i,j)} \\ \vdots & \ddots & \vdots \\ C_{Nh,1}^{(i,j)} & \cdots & C_{Nh,Nb}^{(i,j)} \end{bmatrix} \begin{bmatrix} \Delta I_1 \\ \vdots \\ \Delta I_{Nb} \end{bmatrix}, \quad (9)$$

where N_h is the number of line terminals with healthy conditions.

Equations (5), (6), and (9) are merged to obtain an overdetermined system of equations as below:
$$M = H\theta + \varepsilon$$

$$M = H^J \begin{bmatrix} \Delta J_{i,j} \\ \Delta J_{j,i} \end{bmatrix} + H^I \begin{bmatrix} \Delta I_1 \\ \vdots \\ \Delta I_{Nb} \end{bmatrix}, \quad (10)$$

where M is the data vector and H the observation matrix, the estimated current sources at the faulted line terminals are represented by θ.

The solution is obtained by using the LSE. However, the faulty line identification is carried out by scrutiny of the residuals pertinent to candidate systems of equations. The sum of the vector r is evidently small (ideally zero if measurements are error-free) when the line in question is faulted.

$$\hat{\theta} = \left(H^* H \right)^{-1} H^* M. \quad (11)$$

$$r = M - H\hat{\theta}. \quad (12)$$

C. Third stage: fault distance.

The last stage is regarding computing the fault distance. The fault location formula (13) [16] is used at each superimposed sequence network.

$$\alpha_{i,j} = \frac{\tanh^{-1}}{\kappa_{i,j}} \left(\frac{\cosh(\kappa_{i,j})\Delta V_j - Z_{i,j}^c \sinh(\kappa_{i,j})\Delta J_{j,i} - \Delta V_i}{\sinh(\kappa_{i,j})\Delta V_j - Z_{i,j}^c \cosh(\kappa_{i,j})\Delta J_{j,i} - Z_{i,j}^c\Delta V_i} \right), \quad (13)$$

where $\kappa_{i,j} = \gamma_{i,j}l_{i,j}$, ΔV_j and ΔV_i are the voltage in the faulted line ends.
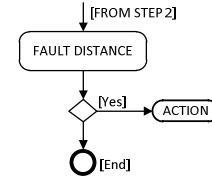

Figure 5. Method flowchart: Third step, fault distance computation

III. STUDY CASES

As a study case, the IEEE-39 bus system is used (see Fig. 5 (a)). The synchrophasors devices or IEDs used to partition the grid into zones are highlighted in red. The border elements must be allocated in buses that genuinely partition the system. For simplicity and reduced phasor data, it is recommended to place them in buses with only two lines, such as bus 25. However, they also can be placed at buses with a high incidence of lines, such as bus 16, where it is necessary to measure a set of phasor voltages and three settings of current phasors. The user could decide the number of elements in each zone based on engineering judgment. In this work, the zones have a similar number of elements. To test the accuracy and robustness of the method, up to 900 different faults are simulated. However, only a single phase to

ground case is presented and analysed in detail due to page limits. This case is associated with an AG fault at 35% of line 13-10, as seen in Fig. 6 (b). Following the steps described in the previous section, the method starts with fault detection. The detection is successfully accomplished at 0.0042 s, as shown in Fig.7.

The delta algorithm is one of the fastest for fault detection in primary protection devices [17]. It was designed to work with time signals. However, here it is used with phasors values. The method proves to be quite efficient, as seen in the pickup reporting of all devices in Fig. 7. All synchrophasors detect the fault successfully, and the farthest one from the fault location is delayed three reporting rates concerning the fault, and the nearest has only one reporting rate.
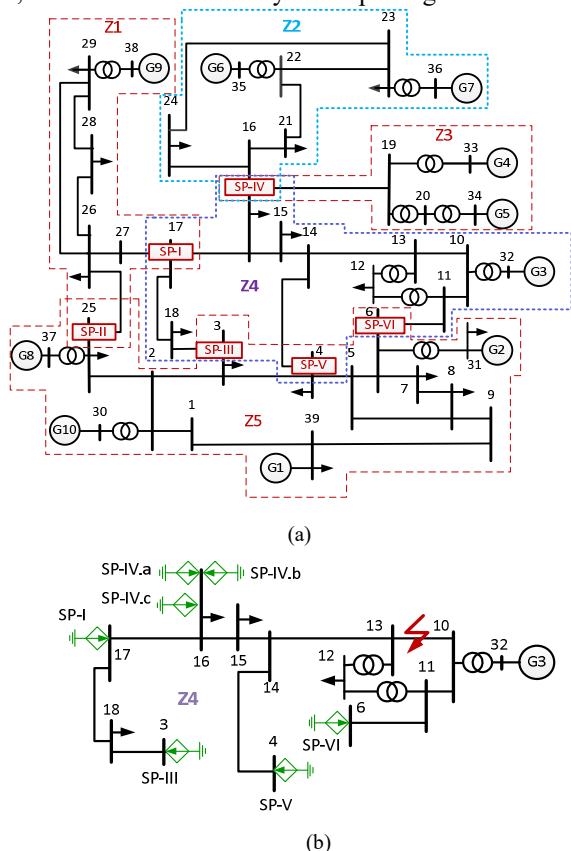

(a)

(b)

Figure 6. Study case (a) Synchrophasor measurement localization and (b) Zone 4, boundaries represented by current sources.
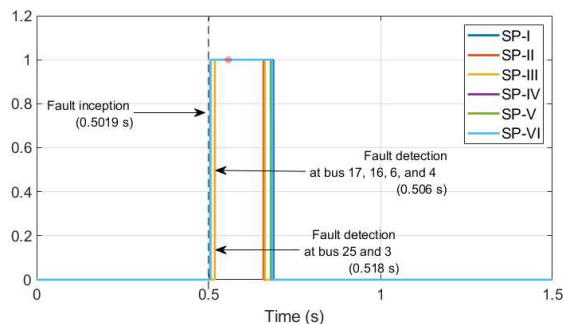

Figure 7. Fault detection times

Fig. 8 shows the response of the faulty phase selection module. All the possible fault combinations are plotted. However, only phase A to ground is active. In Fig. 8, the faulty phase signals are monitored by the synchrophasor of bus 6 (the nearest to the fault). However, synchrophasors at buses 16 and 4 present similar behaviour. The fault is detected at 0.016 s, reporting rate intervals after the fault inception. Therefore, it is not necessary to determine the faulted phase in this stage. However, due to the proposed method's low computation burden, the determination of the faulty phase in this stage becomes efficient.

The direction of the fault is determined by the three different angles below

$$3I^0Z_LV^{1*}, \quad I^2Z_LV^{1*}, \quad and \quad 3I^0I^{2*} \quad (14)$$

where Z_L is the line impedance characteristic angle. For forward faults, the direction characteristic angles (14) must be between $\pi/2$ to π and reverse faults from 0 to $\pi/2$. The direction of the angles at the zone's boundaries determines the faulty zone. An individual truth table is built for each grid under study. The truth table conditions are listed in Table I for the IEEE 39 bus network, which is zoned as shown in Fig. 6 (a). For zone Z4 where the fault takes place, the directions from lines 16-24, 16-21, 16-19, 6-11, 4-14,3-18, and 17-27 (SP-IV.a, SP-IV.b, SP-IV.c, SP-VI, SP-V, SP-III, and SP-I respectively) are as shown in column 5 of Table II. Fig. 9 shows the angle that agrees with zone 4 in Table I.

Once the fault zone is defined, the method builds the corresponding matrices (5), (6) and (7). The LSE is used to obtain the unknowns, and the resulting square residuals determine the faulty line. Fig. 10 shows the behavior of the residuals during a fault. The sum of squared residuals will be as large as 6×10^4 whilst the faulty line has a noticeably small value, such as line 13-10. The detection of the faulty line is done by magnitude comparison and a predefined limit. In this case, from the first residual computation, line 13-10 are lower than the others. Nevertheless, three consecutive steps are needed to determine the faulted line. The load limit proposed in [11] is also implemented here in order to avoid false positives due to load encroachment and heavy load switching.

After the faulty line is determined, the fault distance is calculated by (13). The calculated distance is 33.4% of the line. The average fault distance is estimated with an accuracy of nearly 94%.

TABLE I
IEEE 39 BUS SYSTEM ZONING TRUTH TABLE

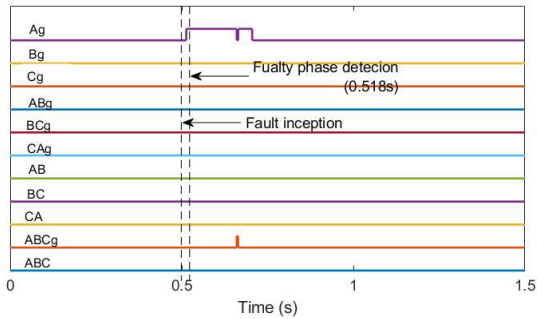| SYNCHROPHASOR	ZONE				
	1	2	3	4	5
SP-I	R			F	
SP-II	F	F			R
SP-IV.a		R		F	
SP-IV.b			R	F	
SP-IV.c				F	
SP-III				F	R
SP-V				R	F
SP-VI				R	F

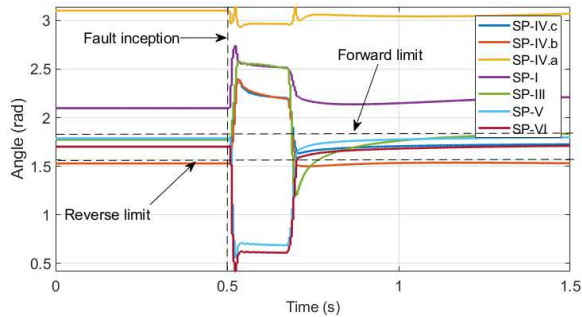Figure 8. Faulty phase selection times at SP-VI (nearest bus to the fault)

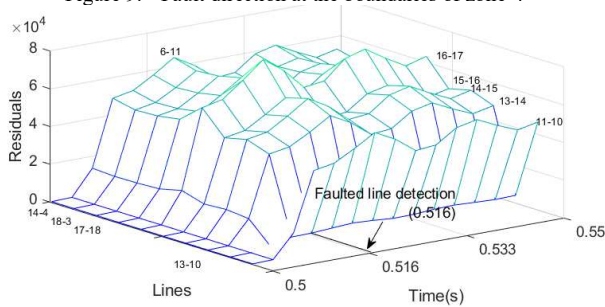Figure 9. Fault direction at the boundaries of zone-4

Figure 10. Residuals used to localize the faulted line

IV. CONCLUSIONS

This paper introduces a comprehensive method for backup protection using synchrophasors data provided by the available PMUs and IEDs. The method comprises three modular stages: 1) fault detection and directionality, 2) faulted zone and faulted line determination, and 3) fault distance. In the first stage, the fault detection, the faulty phase selection, and the directionality are performed. Those indicators are thought to be performed locally at any boundary device. This can alleviate the high computational burden and the amount of data sharing. A truth table is used to determine the faulted zone in the second stage. The data can be received from PMU or IED devices in the control room. To synchronize these data, a rate sampling alteration technique is used. According to the synchrophasor reporting rate, the data obtained from IEDs must be downsampled. After the faulted zone is determined, the LSE is applied with its corresponding square residuals. The faulted line is the one with the least sum of squared residuals. The efficiency of this method was previously tested in [1], [11].

The proposed method is extensively tested through a co-simulation platform built-in RTDS and MATLAB. Local procedures and elements are modelled in RSCAD. A personal desktop computer supplied with MATLAB is connected by Ethernet LAN, a GTNET card, and uses the socket protocol to represent a centralized control room. The modularity of the proposed method gives the user the possibility to change one of the modules for another effective module, if need be.

REFERENCES

[1] S. Azizi, G. Liu, A. S. Dobakhshari and V. Terzija, "Wide-area backup protection against asymmetrical faults using available phasor measurements," *IEEE Trans. in Power Delivery*, vol. 35, no. 4, pp. 2032-2039, August 2020.

[2] A. Sharafi, M. Sanaye-Pasand, and F. Aminifar, "Transmission system wide-area back-up protection using current phasor measurements," *Int. J. Elect. Power Energy Syst.*, vol. 92, pp. 93–103, Nov. 2017.

[3] F. Yu, C. D. Booth, A. Dysko," Voltage-based fault identification for PMU-based wide area backup protection scheme," *IEEE Power & Energy Society General Meeting*, Chicago USA, July 2017.

[4] C. J. Lee, J. B. Park, J. R. Shin, and Z. M. Radojevie, "A new two terminal numerical algorithm for fault location, distance protection, and arcing fault recognition," *IEEE Trans. Power Syst.*, vol. 21, no. 3, pp. 1460-1462, Aug. 2006.

[5] A. G. Phadke, P. Wall, L. Ding, V. Terzija, "Improving the performance of power system protection using wide area monitoring systems," *Journal of Modern Power Systems and Clean Energy*, vol. 4, no. 3, pp. 319-331, July 2016.

[6] G. Kavya, M.M. Devi, and M. Geethanjali, "Wide-area backup protection scheme using optimal PMUs," *National Power Energy Conference*, Madurai India, 2018.

[7] I. Kamwa, A. K. Pradhan, and G. Joos, "Automatic segmentation of large power systems into fuzzy coherent areas for dynamic vulnerability assessment," *IEEE Trans. Power Syst.*, vol. 22, no. 4, pp. 1974-1985, Nov. 2007.

[8] A. S. Dobakhshari, "Wide-area fault location of transmission lines by hybrid synchronized/unsynchronized voltage measurements" *IEEE Trans. Smart Grid*, vol. 9, no. 3, pp. 1869–1877, May 2016.

[9] E. Price and T. Einarsson, "The performance of faulted phase selectors used in transmission line distance applications," *Proc. 2008, 61st Annual Conference for Protective Relays Engineers (CPRE)*, April 2018.

[10] J. Roberts and A. Guzman, "Directional element design and evaluation," *in 21st annual Western protective relay conference*, Washington, 1994.

[11] J. Chavez, N. V. Kumar, S. Azizi, J. L. Guardado, J. Rueda, P. Palensky, V. Terzija, M. Popov, "PMU-voltage drop based fault locator for transmission backup protection," *Electric Power Systems Research*, Vol. 196, pp.1 -8, 2021.

[12] H. León, C. Montez, O. Valle, and F. Vasques, "Real-Time Analysis of Time-Critical Messages in IEC 61850 Electrical Substation Communication Systems, " *Energies*, Vol. 12, no. 12, pp. 1-21, 2019

[13] P. F. Ribeiro, et al. "Power Systems Signal Processing for Smart Grids", John Wiley & Sons, 2013.

[14] S. Azizi and M. Sanayed-Pasand, "A Straightforward method for wide-area fault location on transmission networks," *IEEE Trans. Power Delivery*, vol. 30, no. 1, pp. 264-272, Feb. 2015.

[15] S. Azizi and M. Sanayed-Pasand, "From available synchrophasor data to short circuit fault identity: formulation and feasibility analysis," *IEEE Trans. Power Systems*, vol. 32, no. 3, pp. 2062-2071, May 2017.

[16] A.T. Johns and S. Jamali, "Accurate fault location technique for power transmission lines," *IEE Generation Transmission and distribution*, vol. 137, no. 6 pp. 395-402, Nov. 1990.

[17] P. Horton and S. Swain, "Using superimposed principles (Delta) in protection techniques in an increasingly challenging power network," *in Proc. 2017, 40th Annual Conference for Protective Relay Engineers* (CPRE). April 2017.